Preparation and Properties of a Soluble Polypyrrole−Polypyridyl−Ruthenium(II)−Viologen Dyad

Agnès Martre,[†] Hélène Laguitton-Pasquier,*[,†,‡] Alain Deronzier,*[,†] and Anthony Harriman[§]

Laboratoire d'Electrochimie Organique et de Photochimie Redox, UMR CNRS 5630, Université Joseph Fourier Grenoble 1, BP 53, 38041 Grenoble Cédex 9, France, and Department of Chemistry, Bedson Building, University of Newcastle, Newcastle upon Tyne NE1 7RU, United Kingdom

Received: July 18, 2002; In Final Form: November 25, 2002

Two different kinds of bisviologen-linked $[Ru(bpy)_3]^{2+}$ complexes bearing pyrrole groups were synthesized. We attempt to photopolymerize these dyad systems in the presence of an irreversible oxidative species (O_2 or diazonium salts). The success of the photopolymerization appears to be strongly dependent on the design of the dyad, i.e., the relative arrangement among the $[Ru(bpy)_3]^{2+}$ chromophore, the viologen acceptor, and the polymerizable pyrrole groups. Electrochemical and photophysical characterization of the monomers and of the soluble photopolymer has been made. The intramolecular electron transfer from the ^{3}MLCT excited state of the Ru chromophore to the viologen groups has been evidenced as well as the reverse process. We pay special attention to the photostability of the viologen moieties in the presence of O_2. The photodegradation of the monoreduced viologen in the presence of O_2 provides an emissive species at 546 nm. This photodegradation is not observed in the polymer system. Finally, it has been found that electroreductive precipitation of the photopolymer allows the coating of electrode surfaces with electroactive films exhibiting the redox features of the dyad.

Introduction

Polymers offer the advantage to concentrate in a limited space several active sites of the same molecular system. Considering this remarkable feature, polymer-bound metal complexes hold promise for the design of photoinduced multi-electron-transfer systems. Despite the considerable interest of such molecular assemblies to mimic the natural photosynthesis processes,[1−4] only a few examples involving soluble polymers containing both electron donor or electron acceptor groups and metal complex chromophores on the same polymeric strand are reported.[5−7] Furthermore, although the viologen-linked ruthenium trisbipyridyl complex system has been widely investigated and developed to obtain an efficient charge separation in a thin film or in solution as a monomer, to our knowledge, no soluble polymers with such a dyad system as a pendant group have yet been reported. The only example of soluble polymers containing both ruthenium complexes and viologen moieties has been presented by Matsuo et al.[5] The soluble polymer system they reported results from the copolymerization of two different monomeric units, one bearing a viologen group and the other a ruthenium trisbipyridyl complex.

Two synthetical approaches of such a kind of polymeric assembly can be considered. One is based on the use of preformed polymeric backbones which can be further derivatized by functional molecules. An alternative synthetical route involves the direct polymerization (e.g., electropolymerization) of monomeric structures containing a combination of chromophores, electron-transfer functions, and polymerizable groups.

In the present work, we are focused on the elaboration and the characterization of soluble polymers based on viologen-linked ruthenium trisbipyridyl complex dyads following the second approach. We have recently shown that the photopolymerization and, to less extent, the electropolymerization of pyrrole-substituted ruthenium trisbipyridyl complexes yield to soluble polymers.[8−10] Photopolymerization of those monomers was accomplished in the presence of an irreversible oxidative quencher (O_2 or diazonium salt). This synthetic strategy has been extended to two dyad systems which are covalently linked to pyrrole groups (Chart 1, formulas **1** and **2**). The efficiency of the photopolymerization of those dyads is strongly dependent on their design and especially on the position of the polymerizable group relative to the ruthenium trisbipyridyl complex.

The synthesis and the photophysical and electrochemical characterization of both dyads and of the photopolymer of dyad **2** are described in the present paper. The results are compared to those obtained on complexes not bearing viologen units (formulas **3**−**5**, Chart 1).

Experimental Section

A. Materials. Methyl viologen hexafluorophosphate (MV^{2+}) was obtained by converting methyl viologen dichloride (Fluka) to the PF_6^- salt using an ion exchange column containing Amberlite IRA-93 ion exchanger in the hexafluorophosphate form. Tetra-*n*-butylammonium perchlorate (TBAP) obtained from Fluka was dried under vacuum at 80 °C for 72 h. Acetonitrile used in photophysical measurements was spectrophotometric grade (SDS). Acetonitrile used in the synthesis and in electrochemical measurements was HPLC grade (Rathburn).

* To whom correspondence should be addressed. Phone: + 33 476 635706. Fax: + 33 476 514267. E-mail: alain.deronzier@ujf-grenoble.fr (A.D.); helene.laguitton-pasquier@lcp.u-psud.fr (H.L.-P.).

† Université Joseph Fourier Grenoble 1.

‡ Present address: Laboratoire de Chimie Physique, UMR CNRS 8000, Université de Paris-Sud, Bat. 350, 91405 Orsay Cédex, France.

§ University of Newcastle.

10.1021/jp021645j CCC: $25.00
Published on Web 03/06/2003

CHART 1: Structure of the Pyrrole-Substituted Ruthenium(II) Bisviologen-Linked Dyads 1 and 2 and of the Model Compounds 3−5 Investigated

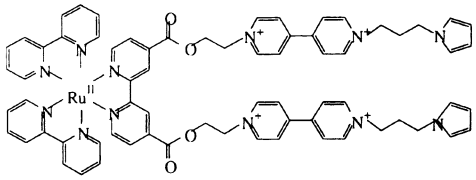

$[Ru(bpy)_2(L_1)]^{6+}$ **1**

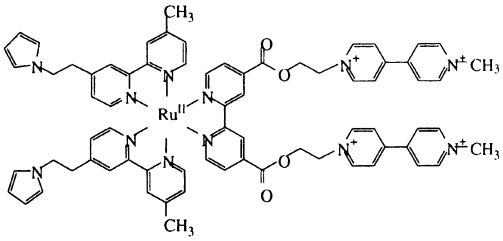

$[Ru(L_3)_2(L_2)]^{6+}$ **2**

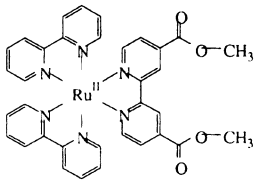

$[Ru(bpy)_2(L_4)]^{2+}$ **3**

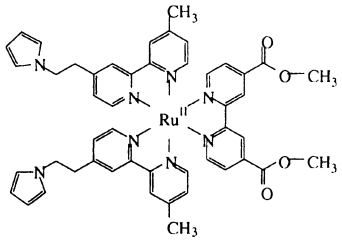

$[Ru(L_3)_2(L_4)]^{2+}$ **5**

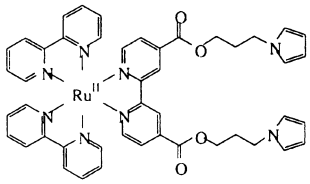

$[Ru(bpy)_2(L_5)]^{2+}$ **4**

B. Compound Synthesis. *B.1. Ligands.* 2,2′-Bipyridine (bpy; Aldrich, 99%) was used as received. The ligands L_1, L_3, L_4, and L_5 were synthesized as previously described.[11−14]

Ligand L_2 was prepared by a method similar to that of L_1[11] by refluxing for 1 h 144 mg (0.51 mmol) of 4,4′-dichloroformyl-2,2′-bipyridine with 398 mg (1.02 mmol) of 1-methyl-1′-(2-hydroxy-1-ethyl)-4,4′-bipyridine ditetrafluoroborate in CH_3CN (5 mL) in the presence of collidine (100 μL). The cooled reaction mixture was evaporated under vacuum, and the precipitate was dissolved in a CH_3CN/H_2O (3:1) mixture and passed through an ion exchange column (Amberlite IRA-93) in BF_4^- form. The product obtained after the solvent was evaporated was dried, then redissolved in a minimum of CH_3CN, and precipitated by addition of CH_2Cl_2. This procedure was repeated once. Yield: 71% (352 mg).

^{1}H NMR (CD_3CN): δ 9.06 (m, 4H); 8.83 (m, 8H); 8.47 (m, 4H); 8.39 (m, 4H); 7.88 (m, 2H); 5.08 (t, 4H); 4.49 (t, 4H); 4.39 (s, 6H).

B.2. Complexes. Precursor complexes $Ru(bpy)_2Cl_2 \cdot 2H_2O$ and $Ru(L_3)_2Cl_2 \cdot 2H_2O$ were prepared following a litterature procedure.[15,16]

$[Ru(bpy)_2(L_1)](BF_4)_6$ (**1**) was prepared and characterized (FAB-MS) as reported earlier.[11]

^{1}H NMR (CD_3CN): δ 9.09 (m, 2H); 9.07 (m, 2H); 8.90 (m, 2H); 8.79 (m, 2H); 8.76 (m, 2H); 8.50 (m, 2H); 8.48 (m, 2H); 8.47 (m, 2H); 8.45 (m, 2H); 8.33 (m, 2H); 8.30 (m, 2H); 8.07 (m, 2H); 8.03 (m, 2H); 7.95 (m, 2H); 7.79 (m, 2H); 7.69 (m, 2H); 7.66 (m, 2H); 7.41 (m, 2H); 7.35 (m, 2H); 6.63 (s, 4H); 5.97 (s, 4H); 5.09 (m, 4H); 4.86 (m, 4H); 4.59 (m, 4H); 4.07 (m, 4H); 2.51 (m, 4H).

$[Ru(L_3)_2(L_2)](BF_4)_6$ (**2**) was synthesized by a method similar to that of **1**. A solution of L_2 (0.125 g, 0.127 mmol) and $Ru(L_3)_2Cl_2 \cdot 2H_2O$ (0.111 g, 0.159 mmol) in 20 mL of H_2O/*tert*-butyl alcohol (50:50) was heated at reflux for 3 h under argon in the absence of light. The cooled reaction mixture was filtered to remove the slight excess of $Ru(L_3)_2Cl_2 \cdot 2H_2O$. The ruthenium complex was then precipitated from the solution by addition of concentrated NH_4PF_6. The red-brown precipitate was collected by filtration. Purification was acheived by precipitation from an acetone solution by slow addition of diethyl ether (143 mg, yield 63%). UV −vis: λ_{max} (in CH_3CN) = 490 nm.

^{1}H NMR (CD_3CN): δ 9.11 (m, 2H); 9.08 (m, 2H); 8.87 (m, 2H); 8.86 (m, 2H); 8.82 (m, 2H); 8.52 (m, 2H); 8.47 (m, 2H); 8.36 (m, 2H); 8.33 (m, 2H); 8.17 (m, 1H); 8.15 (m, 1H); 7.92 (m, 1H); 7.91 (m, 1H); 7.87 (m, 1H); 7.85 (m, 1H); 7.81 (m, 1H); 7.77 (m, 1H); 7.42 (m, 2H); 7.36 (m, 2H); 7.26 (m, 1H); 7.16 (m, 1H); 7.08 (m, 1H); 7.01 (m, 1H); 6.55 (d, 2H); 6.45 (d, 2H); 5.87 (d, 2H); 5.84 (d, 2H); 5.09 (m, 4H); 4.86 (m, 4H); 4.40 (s, 6H); 4.19 (m, 2H); 4.13 (m, 2H); 3.19 (m, 2H); 3.13 (m, 2H); 2.53 (s, 3H); 2.48 (s, 3H).

FAB-MS: *m*/*z*, positive mode, (M^{6+}, $5BF_4^-$) 1703, (M^{6+}, $4BF_4^-$) 1616, (M^{6+}, $3BF_4^-$) 1529, (M^{6+}, $2BF_4^-$) 1441.

$[Ru(bpy)_2(L_4)](PF_6)_2$ (**3**), $[Ru(bpy)_2(L_5)](PF_6)_2$ (**4**), and $[Ru(L_3)_2(L_4)](PF_6)_2$ (**5**) were prepared and purified following the general method described in ref 16.

(**3**) UV−vis: λ_{max} (in CH_3CN) = 490 nm.

^{1}H NMR (CD_3CN): δ 9.02 (s, 2H); 8.50 (m, 2H,); 8.49 (m, 2H); 8.08 (m, 2H); 8.06 (m, 2H,); 7.93 (m, 2H); 7.81 (m, 2H); 7.69 (m, 2H); 7.64 (m, 2H); 7.42 (m, 2H); 7.37 (m, 2H); 3.9 (s, 6H).

FAB-MS: *m*/*z*, positive mode, (M^{2+}, PF_6^-) 831, (M^{2+}) 686.

(**4**) UV−vis: λ_{max} (in CH_3CN) = 490 nm.

^{1}H NMR (CD_3CN): δ 8.91 (s, 2H); 8.52 (m, 2H); 8.50 (m, 2H); 8.09 (m, 2H); 8.07 (m, 2H,); 7.91 (m, 2H); 7.80 (m, 2H); 7.70 (m, 2H); 7.66 (m, 2H); 7.42 (m, 2H); 7.39 (m, 2H); 6.69 (m, 4H); 5.96 (m, 4H); 4.34 (t, 4H, J = 6.4 Hz); 4.07 (t, 4H, J = 6.4 Hz); 2.23 (quintet, 4H, J = 6.4 Hz).

FAB-MS: *m*/*z*, positive mode, (M^{2+}, PF_6^-) 1017, (M^{2+}) 872.

(**5**) UV−vis: λ_{max} (in CH_3CN) = 490 nm.

^{1}H NMR (CD_3CN): δ 8.99 (s, 2H); 8.19 (m, 1H); 8.16 (m, 1H); 7.96 (m, 1H); 7.93 (m, 1H); 7.88 (m, 2H); 7.80 (m, 2H); 7.41 (m, 2H); 7.26 (m, 1H); 7.17 (m, 1H); 7.08 (m, 1H); 7.01 (m, 1H); 6.54 (m, 4H); 5.94 (m, 4H); 4.19 (m, 4H); 3.98 (s, 6H); 3.18 (m, 4H); 2.53 (s, 3H); 2.50 (s, 3H).

FAB-MS: *m*/*z*, positive mode, (M^{2+}, PF_6^-) 900.

C. Polymer Synthesis. Photopolymers were synthesized from millimolar solutions of pyrrole-substituted dyads in aerated acetonitrile with the light of a 250 W Hg lamp filtered through UV and IR cutoff filters following a procedure similar to that previously described for the simplest pyrrole−$Ru(bpy)_3^{2+}$ complexes.[8] The resulting soluble functionalized polypyrrole from dyad **2** (photopoly-**2**) was obtained in its overoxidized form. This has been evidenced by IR spectroscopy of the polymers, which exhibit carbonyl bands typical of the presence of some pyrrolidone moeties,[17] and by the lack of polypyrrole electroactivity in cyclic voltammetry.[8,9] Furthermore, any absorption of the polypyrrole backbone has been detected in the UV−vis part.

All attempts to characterize the average molecular weight of the polymers using GPC or light scattering experiments were unsuccessful.

D. Sample Preparation. The complex concentration was typically 1.5×10^{-3} M for electrochemical experiments and 5×10^{-6} M for stationary experiments (absorption and emission spectra, emission quantum yield determination). Due to the weak luminescence of the Ru complexes, the decay curves of the model compounds have been recorded on samples of 5×10^{-5} M to obtain the best signal-to-noise ratio.

All solutions were freshly prepared prior to use in an inert atmosphere (Ar) glovebox. All the photophysical experiments were performed at 25 °C in CH_3CN on deoxygenated solutions (Ar atmosphere, sealed cells) except where otherwise stated. All electrochemical measurements were recorded under an argon atmosphere at room temperature.

E. Apparatuses. The electrochemistry measurements in CH_3CN/TBAP electrolyte were done with a PAR 273 electrochemical system. The working electrode consisted of a 5 mm diameter platinum or vitreous carbon disk polished with 1 μm diamond paste (Mecaprex Presi PM) for analytical experiments. Large-scale electrolyses were performed on a platinum plate (8 cm^2). Potentials are reported relative to the Ag^+ (10^{-2} M)/Ag reference electrode. The surface coverage (Γ) of immobilized complexes on the electrode surface was determined from the charge recorded at low scan rates under the Ru(II) → Ru(III) oxidation peak.

Proton NMR spectra were recorded at 25 °C on a Varian Unity 500 MHz spectrometer with the compounds dissolved in CD_3CN.

UV−vis spectra were obtained using a Cary 1 absorption spectrophotometer with 1 cm path length quartz cells. The steady-state emission spectra were recorded on a Photon Technology International (PTI) SE-900M spectrofluorimeter. The emission quantum yield ϕ_L was determined at 25 °C in deoxygenated acetonitrile solutions.

Time-resolved studies, recorded on the model compounds, were performed on a PTI Quanta-Master luminescence lifetime spectrometer. It consists of a nanosecond flash lamp coupled to a lens-based T-format sample compartment that has a stroboscopic detector. The detailed description of the instrument has been previously reported.[18] To obtain the best signal-to-noise ratio, the decay curves have been performed under excitation over the wavelength window 300−450 nm and using a 475 nm cutoff filter which screened scattered lamp light. We checked that the decay curves did not depend on the excitation wavelengths (300−450 nm). Decay curves were obtained by monitoring at 650 nm. No systematic variation in the characteristics of the decay curves was found in the 580−800 nm range. Flash pulses scattered from a nonfluorescing CH_3CN solution in a 1 cm path length quartz cell were used to generate the instrument response function. The decay curves were analyzed by using PTI software based on iterative reconvolution using a Marquardt algorithm.[19] The accuracy of the fit was evaluated by inspecting the residuals.

Luminescence lifetime measurements for dyad **1** and dyad **2** as well as laser flash photolysis studies were made using the setup described earlier.[20]

Results and Discussion

A. Monomers. *A.1. NMR Studies.* All signals were assigned by the use of homonuclear correlation (COSY) and of nuclear Overhauser effect (NOESY) two-dimensional experiments. The ^{1}H NMR data of dyad **1** and of the corresponding model complexes indicate the inequivalence in the complex of the two halves of each of the symmetrical unsubstituted bipyridine ligands (Figure 1S in the Supporting Information). This results from the fact that the two halves of each bpy are oriented over the plane of the two different adjacent ligands, the second bpy, and the ester-substituted bipyridine ligand, which induces magnetically inequivalent environments. In the case of dyad **2** (Figure 1S) and of complex **5**, there is a further complication. Due to the unsymmetrical nature of the ligand L_3, there are three possible geometric isomers[21] based on the relative orientation of the alkylpyrrole moiety. This induces a split of most of the proton resonances. As an example, the α-protons of the pyrrol groups exhibit at least two different resonances which are separated by 0.1 ppm.

On the other hand, while the proton resonances of the alkyl chain of the two halves of the viologen-substituted bipyridine ligand are identical, all the proton resonances associated with the viologen groups are slightly split so that they appear to be under two magnetically distinguished environments. As this trend is observed for both dyads, it is independent of the nature of the two other bpy ligands of the complex. This behavior can result from the upfield shift of the protons of a viologen unit which are under the out-of-plane ring current of the neighboring viologen. Furthermore, from NOESY experiments, no specific intramolecular interactions, for instance, interaction between the two viologen moieties, occur in the dyad systems at room temperature, which is in agreement with the fact that the splitting of the proton resonances of the viologens is slight.

Since the isomers of complexes **2** and **5** are expected to exhibit close photophysical and electrochemical properties, no attempts were made to separate those isomers.

A.2. Electrochemistry. Dyads **1** and **2** have identical electrochemical behavior in acetonitrile/0.1 M TBAP. Figure 1 shows their representative cyclic voltammogram at a Pt and carbon electrode, which exhibits six reduction waves and one oxidation one. The two reversible two-electron waves of the viologen groups are followed by four reversible one-electron waves due to the reduction of the bipyridine ligands. The first and the last ones are attributed to the two succesive reductions of the bpy ligand substituted by the ester group, while the second and the third ones are attributed to the reduction of the two regular bipyridyne ligands. The $E_{1/2}$ values of the ligand-centered reduction of the dyads are close to those of the model complexes **3**−**5** not containing the viologen moieties; see Table 1 for those data. Note that some adsorption−desorption phenomena are seen

TABLE 1: Electrochemical Data for Monomer Complexes and Photopoly-2-Modified Electrodes

	oxidation	reduction					
complex	$E^7_{1/2}$	$E^1_{1/2}$	$E^2_{1/2}$	$E^3_{1/2}$	$E^4_{1/2}$	$E^5_{1/2}$	$E^6_{1/2}$
$[Ru(bpy)_2(L_4)]^{6+}$, dyad **1**	1.00	−0.66	−1.10	−1.25	−1.73	−1.92	−2.20
$[Ru(L_1)_2(L_5)]^{6+}$, dyad **2**	1.00	−0.70	−1.14	−1.30	−1.77	−2.08	−2.35
$[Ru(bpy)_2(L_6)]^{2+}$, **3**	1.08			−1.27	−1.72	−1.91	−2.18
$[Ru(bpy)_2(L_7)]^{2+}$, **4**	1.08			−1.27	−1.74	−1.92	−2.20
$[Ru(L_1)_2(L_6)]^{2+}$, **5**	1.06			−1.32	−1.81	−2.02	−2.28
photopoly-**2** (O_2)	0.98	−0.67	−1.13	−1.28	−1.81	−2.01	−2.32
photopoly-**2** (ArN_2^+)	1.00	−0.66	−1.11	−1.26	*a*	*a*	*a*

[a] Not determined. Ill-defined waves.

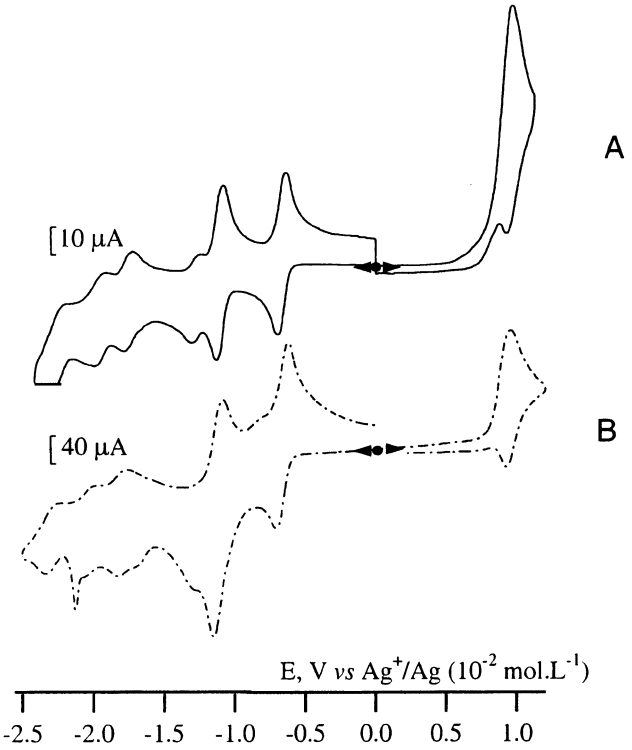

Figure 1. Cyclic voltammogram in CH_3CN/0.1 M TBAP, sweep rate $\nu = 100$ mV s^{-1}, (A) at a C electrode of a 1.5 mM solution of **1** and (B) at a Pt electrode of a 1.5 mM solution of **2**.

for dyad **2** on a Pt electrode. In the anodic region the Ru^{2+}/Ru^{3+} wave is melted with the irreversible oxidation of the pyrrole group as observed for regular tris(bipyridine)ruthenium-(II) complexes containing pyrrole substituents.[12]

As previously reported for dyad **1**,[11] modified electrodes can be easily prepared by repeatedly scanning the potential over the range from 0 to 1.2 V. Figure 2 shows a typical cyclic voltammogram of a resulting thin film of poly-**2** for instance. All the reversible redox couples of the reduction of the bpy ligand are clearly observed as well as that of the Ru^{2+} oxidation, associated with a prepeak due to some change of the resistivity of the film.[22] These thin films can also be prepared by potentiostating the electrode at 0.75 V. Exhaustive electrolysis carried out at 0.90 V does not produce any soluble species; poly-**1** and poly-**2** are fully insoluble and coated on the platinum gauze foil electrode.

A.3. Photophysics. The absorption spectra of both dyads and of the model complexes consist of MLCT ($d\pi \rightarrow \pi^*$) and interligand ($\pi \rightarrow \pi^*$) bands, typical for polypyridyl complexes of ruthenium(II).[23,24] Especially, the broad band observed in the visible region results from the overlap of the $d\pi(Ru) \rightarrow \pi^*$-(bpy) and $d\pi(Ru) \rightarrow \pi^*(bpy(COOMe)_2)$ charge-transfer transitions, respectively, at 450 and 476 nm.[25] On the other hand, in

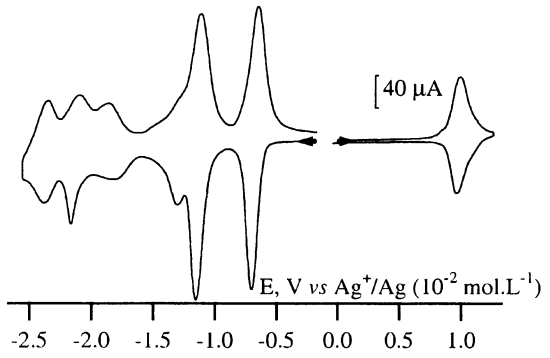

Figure 2. Cyclic voltammogram in CH_3CN/0.1 M TBAP, sweep rate $\nu = 100$ mV s^{-1}, of a Pt/poly-**2**-modified electrode ($\Gamma = 1.6 \times 10^{-8}$ mol·cm^{-2}).

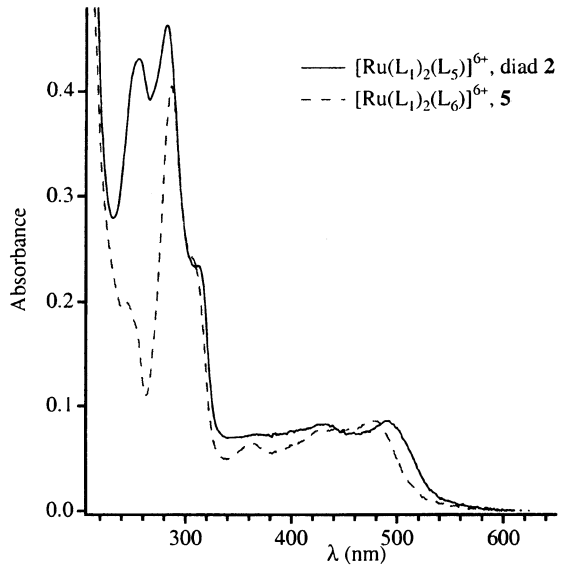

Figure 3. Absorption spectra of dyad **2** and of the model compound **5** in deoxygenated acetonitrile solution at 25 °C.

addition to the specific absorption spectra of the Ru(II) chromophore, the covalently linked viologen−Ru(II) complexes exhibit a supplementary band at 250 nm due to the viologen moieties[26] (Figure 3). It should be noted that, for both dyads, there is no indication of specific electronic interactions between the Ru(II) chromophore and the viologen moieties in the ground state, corroborating the NMR studies.

The broad and structureless emission spectra of complexes **1**−**5** are characteristic of MLCT transitions.[24,25] As the emission spectra do not depend on the excitation wavelengths (300−500 nm), the excitation leads to the rapid population of the lowest energy ^{3}MLCT level. The emitting state is localized on the bpy ligand having the lowest π^*-acceptor orbital energy,[25,27−29] which is the bipyridine ligand substituted with the electron-withdrawing ester groups.

TABLE 2: MLCT Absorption Band Maxima (λ_{abs}^{max}), Luminescence Maxima (λ_{em}^{max}), and Luminescence Decay Times (τ) for Dyads 1 and 2 and the Model Compounds 3 and 5 at 298 K in Deoxygenated Acetonitrile Solution[a]

complex	λ_{abs}^{max} (nm)	λ_{em}^{max} (nm)	ϕ_{dyad}/ϕ_{model}	τ (ns)	k_{CT} (s^{-1})	k_b (s^{-1})
$[Ru(bpy)_2(L_4)]^{6+}$, dyad **1**	476	666	0.01	1.55	6.4×10^8	3.5×10^9
$[Ru(bpy)_2(L_6)]^{2+}$, **3**	478	668	1	750		
$[Ru(L_1)_2(L_5)]^{6+}$, dyad **2**	490	677	0.01	1.62	6.2×10^8	3.5×10^9
$[Ru(L_1)_2(L_6)]^{2+}$, **5**	478	668	1	1080		

[a] The emission quantum yield of both dyads relative to that of their corresponding model compounds (ϕ_{dyad}/ϕ_{model}) is indicated. The rate constants for the forward (k_{CT}) and the back (k_b) intramolecular electron-transfer processes in dyads **1** and **2** are presented.

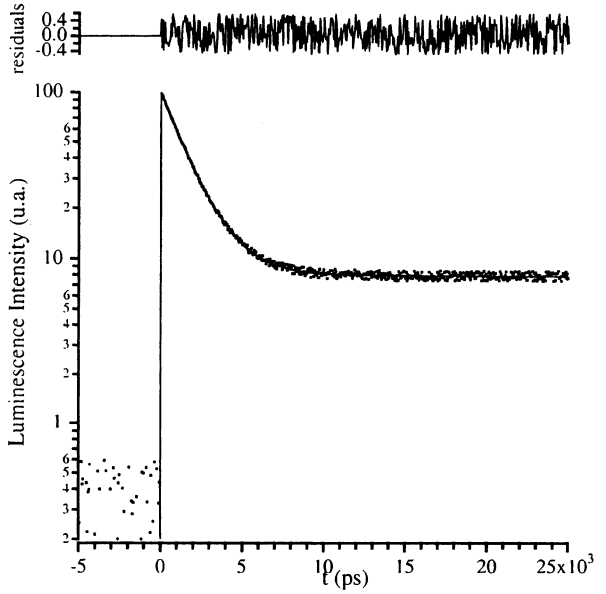

Figure 4. Emission decay curve recorded at 660 nm for dyad **2** in deoxygenated acetonitrile solution at 25 °C. Shown with the experimental curve are the best fit to a single exponential and the resulting residuals.

A.3.a. Forward Electron-Transfer Process. The luminescence quantum yield and time decay of both covalently linked Ru(II)−viologen complexes are significantly disminished in comparison to that of the model complexes (Table 2). Whereas the lifetime of the model compounds is close to 800 ns, that of both dyads amounts to 1.6 ns (Figure 4, Table 2). This evidences the quenching by the covalently linked viologen groups, which can be ascribed to the intramolecular electron transfer from the excited Ru(II) complex to the viologen units.[30] This is supported by the observation of the characteristic differential absorption spectrum of the monoreduced viologen at 600 nm (Figure 5). From the measured excited-state lifetimes of the covalently linked Ru(II)−viologen complex (τ) and of the corresponding model complex (τ_{ref}), the rate constant for the intramolecular electron transfer k_{CT} can be estimated according to

$$k_{CT} = \frac{1}{\tau} - \frac{1}{\tau_{ref}} \qquad (1)$$

The values of k_{CT}, given in Table 2, amount to around 6×10^8 s^{-1} for both dyads. They are consistent with those reported in the literature for analogous systems. Kelly and Rodgers[29] have investigated viologen-linked ruthenium(II) complexes with different methylene chain lengths between the ruthenium complex and the viologen unit: $Ru(bpy)_2(4\text{-}CH_3\text{-}2,2'\text{-bipyridine-}4'\text{-}(CONH{-}(CH_2)_x{-}V^{2+}{-}CH_3))$ designated by 1−*x*−MV. The forward electron-transfer rates in the 1−2−MV and 1−3−MV systems were, in CH_3CN, 2.9×10^{10} and 4.1×10^8 s^{-1}, respectively. Hiraiski et al.[31] have investigated similar systems: $Ru(bpy)_2(dcbpy)(C_mVC_n)$, where dcbpy denotes the 4-carboxy-2,2′-bipyridine-4′-carbodiimide ligand, C_m and C_n denote the methylene chains, and V denotes the viologen moiety. The intramolecular electron-transfer rate appears to be less dependent on the ruthenium−viologen distance since it amounted to 2.54×10^8 and 2.68×10^8 s^{-1}, respectively, for the $Ru(bpy)_2(dcbpy)C_2VC_3$ and $Ru(bpy)_2(dcbpy)C_3VC_4$ systems. On the other hand, Yonemoto et al.[32] have studied the dependence of the donor−acceptor separation distance in a series of covalently linked Ru(II)−viologen systems on the rate of the photoinduced forward electron transfer. The linkage between the tris(bipyridyl)ruthenium(II) complex and the viologen group was an alkyl chain branched on the 4′-position of the 2,2′-bipyridine ligand. The rate constants for the intramolecular electron transfer varied exponentially with the number of methylene units ($n = 1-5$) and amounted to, in CH_3CN, 7.9×10^9, 2.0×10^9, 6.5×10^8, and 6.5×10^7 s^{-1} for $n = 2$, 3, 4, and 5, respectively. The system having $n = 4$ and dyads **1** and **2**, which may be comparable in donor−acceptor distance, exhibit quite similar values.

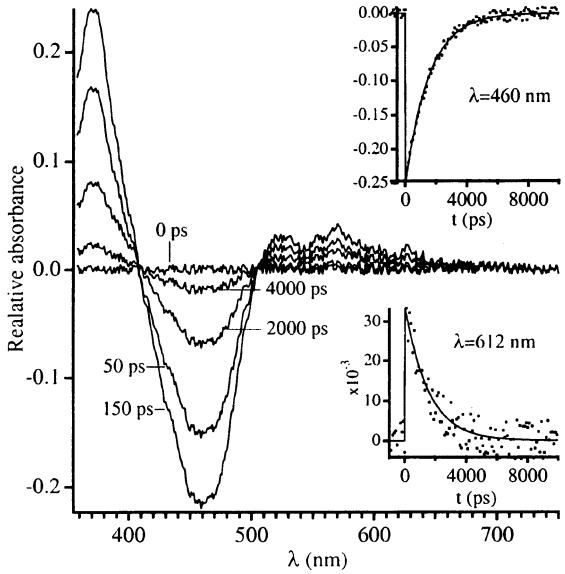

Figure 5. Transient absorption spectra for dyad **2** in deoxygenated acetonitrile solution at 25 °C recorded 0−4000 ps after 532 nm laser excitation. The insets show the rapid rise and decay of the $V^{\bullet+}$ signal at 612 nm as well as the recovery of the ground state $[Ru(bpy)_3]^{2+}$ at 460 nm. The solid line is the best fit to the data.

Furthermore, Matsuo et al.[5] have reported a dyad system analogous to those investigated here since two viologen units are covalently linked to a tris(2,2′-bipyridine)ruthenium(II) complex via an amide substitution at the 4- and 4′-positions of one 2,2′-bipyridine and an alkyl chain linking the viologen. From the values of the luminescence quantum yields they reported for the systems $2C_2V^{2+}C_{2-}Ru^{2+}$ and $2C_{16}V^{2+}C_{2-}Ru^{2+}$ in which Ru^{2+} denotes the $Ru(bpy)_2(bpy(CONH{-})_2)$ complex and C_n an alkyl chain constituted by *n* methylene units, we estimate the rate constants of intramolecular electron transfer for those two systems to be 2.89×10^7 and 2.78×10^8 s^{-1}, respectively. Those values are determined assuming that the lifetime of the complex without viologen units is similar to that reported by Kelly and Rodgers[29] for the $Ru(bpy)_2(4\text{-}CH_3\text{-}2,2'\text{-bipyridine-}4'\text{-}CONHCH(CH_3)_2)$ complex (τ = 595 ns at 22 °C in CH_3CN). The difference between those two values of intramolecular electron-

transfer rate constant is perhaps not so significant since the quantum yields are very low and probably of the same order of the experimental error.

Despite an imperfect match of the values of the intramolecular electron-transfer rate obtained for the various Ru(II)−viologen dyad systems reported in the literature or by us, the rate constants for systems comparable in donor−acceptor separation distance are of the same order. The nature of the donor−acceptor linkage can explain partly the difference observed as one can assume that, for such donor−acceptor distances, the electron-transfer mechanism is mainly through-bond. But the nature of the substituent branched on the 4-position of the 2,2′-bipyridine bearing the viologen unit as well as the number of viologen units per complex can also contribute, probably to less extent, to the difference observed. On the other hand, it seems that the presence of two viologen units on the same bpy ligand did not modify or at the most shortened slightly the rate constant for forward electron transfer with respect to systems bearing only one viologen moiety. This rules out specific interactions between the viologen units.

A.3.b. Back-Electron-Transfer Process. On the other hand, following the forward electron-transfer process, the disappearance of the absorbance of the monoreduced viologen at 600 nm concommitent with the bleaching recovery of the Ru ground state at 450 nm (Figure 5) evidences the reverse electron-transfer process. As observed in Figure 5, the monoreduced viologen species is present in a very low yield compared to the MLCT excited state of the Ru chromophore. It points out that the charge recombination process is faster than the forward electron transfer. Extraction of the reverse electron-transfer rate constant, k_b, was accomplished by fitting the observed absorbance change at 612 nm in the framework of eq 2, where $[^3\text{MLCT*}]_0$

$$[V^{\bullet+}] = [^3\text{MLCT*}]_0 \frac{k_{CT}}{k_b - k_{CT}}(e^{-k_{CT}t} - e^{-k_b t}) \qquad (2)$$

represents the initial concentration of the emissive ^{3}MLCT excited state. For each dyad,[30] the reverse electron-transfer rate constant was estimated to be $3.5 \times 10^9\ s^{-1}$. That value is similar to that reported in the literature. The rate constants of the back electron tranfer for the 1−2−MV and 1−3−MV systems studied by Kelly et al.[29] were estimated to be, respectively, 4.8×10^9 and $6.1 \times 10^9\ s^{-1}$. The value reported by Yonemoto et al.[32] amounts to $3.2 \times 10^9\ s^{-1}$ for a system bearing four methylene units between the Ru chromophore and the viologen group.

B. Photopolymerization. We have previously demonstrated that photopolymerization of pyrrole-substituted ruthenium tris-bipyridyl complexes can be accomplished in the presence of an irreversible oxidative quencher (O_2 or diazonium salts).[8−10] The Ru(III) species formed upon intermolecular electron-transfer quenching of the excited state oxidized the pyrrole moieties. A similar phenomenon can be expected with dyads **1** and **2**. However, the presence of the covalently linked viologen moieties can interfere with the process since we have seen that the latter act as an intramolecular quencher of the Ru^{2+}* excited state. Moreover, with O_2 as external quencher, some degradation of the dyads can occur since the photogenerated $O_2^{\bullet-}$ species reacts with viologen.[33]

The photopolymerization is followed by ^{1}H NMR experiments conducted in deuterated acetonitrile solutions of the dyad and O_2 or diazonium salts. For dyad **2**, at the end of the photolysis, the aromatic resonances of the H atoms of the pyrrole moieties have totally desappeared. Furtheremore, all the proton resonances of the photopolymer poly-**2** are much broader than those of the corresponding monomer, dyad **2**, which is generally observed for polymer proton NMR[34] (see Figure 6 for irradiation of dyad **2** in the presence of molecular oxygen, duration 4 h). On the other hand, signals due to the protons of the viologens remain unchanged, showing that the viologen structure in the dyad is kept.

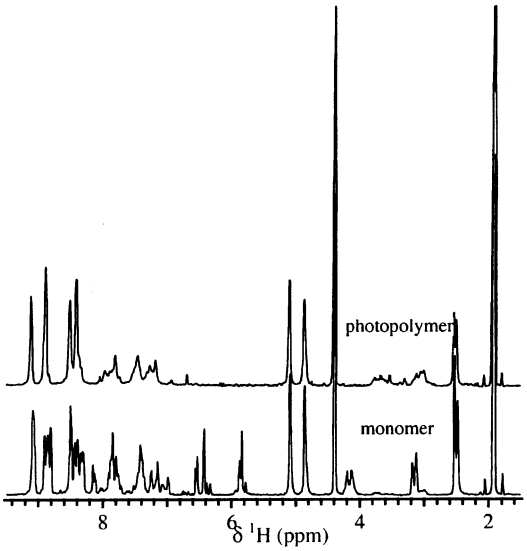

Figure 6. ^{1}H NMR spectra of the monomer and of the photopolymer (obtained in the presence of the irreversible oxidative quencher O_2) of dyad **2** at 500 MHz and 25 °C in CD_3CN solution.

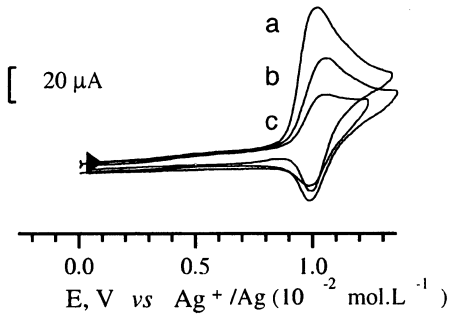

Figure 7. Evolution of the cyclic voltammogram in CH_3CN/0.1 M TBAP, sweep rate $\nu = 100$ mV s^{-1}, at a Pt electrode of a 0.9 mM aerated solution of **2**, during irradiation at $\lambda > 405$ nm: (a) $t = 0$; (b) $t = 10$ min; (c) $t = 36$ min.

This photopolymerization process could also be followed by cyclic voltammetry experiments. The Ru(II/III) couple becomes more reversible after visible irradiation under air or in the presence of diazonium salts (Figure 7). No wave corresponding to the regular polypyrrole electroactivity is detected. The polypyrrole matrix is overoxidized during the photopolymerization process as a consequence of the strong oxidizing power of the photogenerated Ru(III) species. No precipitate is detected, indicating that the photopoly-**2** is fully soluble in contrast to the electrochemically prepared one (see above).

In contrast, photopolymerization of dyad **1** does not occur in the presence of either O_2 or a diazonium salt. The cyclic voltammograms and NMR spectra are identical after photolysis. However, for the latter technique, some changes are observed in the pattern of the protons of the viologen part, indicating some degradation which can also be evidenced by luminescence experiments.

Degradation of the Viologen Units in the Presence of Oxygen. The emission spectrum of a CH_3CN solution of dyad **1**

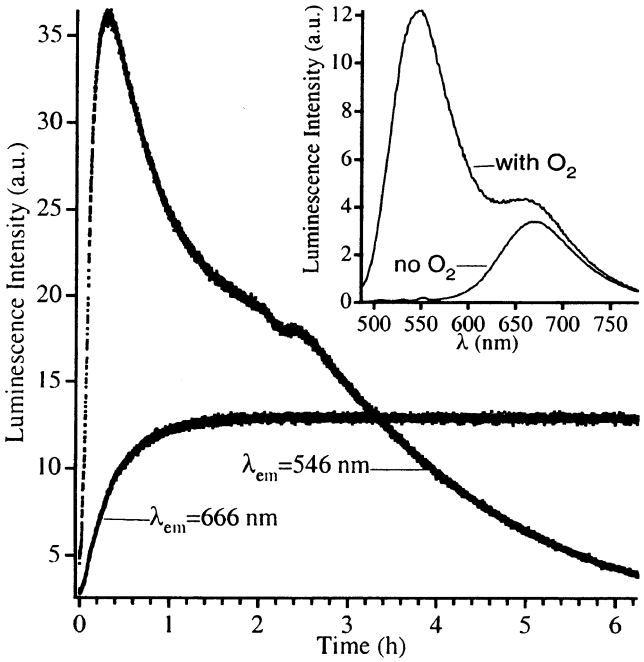

Figure 8. Evolution of the luminescence intensity of dyad **1** in acetonitrile solution containing air at 546 and 666 nm. The inset shows the emission spectrum (λ_{ex} = 470 nm) at 25 °C of an acetonitrile solution of dyad **1** in the presence or absence of O_2.

containing air has been performed before and after irradiation at 476 nm. Whereas the emission spectrum of the nonirradiated solution exhibits the typical band at 666 nm caracteristic of the emission of dyad **1**, after irradiation, a supplementary band appears at 546 nm (Figure 8, inset). The emission intensity at 546 nm increases quickly and then decreases as a function of the time of irradiation, while that at 666 nm increases progressively up to a plateau (Figure 8). Furthermore, the decay time of dyad **1**, estimated to be a few nanoseconds before irradiation, amounts to 900 ns after irradiation. Those observations indicate the disappearance of the quenching by the viologen moieties of the excited ruthenium complex and suggest the decomposition by O_2 of the viologen units.

Similar experiments were performed on a CH_3CN/0.1 M TBAP solution of the radical cation of methyl viologen, $MV^{\bullet+}$, prepared in a glovebox by electrolysis at −0.9 V. In the absence of oxygen, the $MV^{\bullet+}$ solution is characterized by an absorption band at 284 nm and an emission band at 325 nm (Figure 9). The intensity of emission at 325 nm is independent of the time of irradiation. In the presence of oxygen, a new emission band appears at 535 nm, the excitation spectrum of which is similar to that obtained for the aerated solution of dyad **1** at 546 nm.[35] Furthermore, the emission intensities of the bands at 535 and 546 nm behave similarly as a function of the time of irradiation in the presence of O_2 (Figure 9, inset): the formation of a fluorescent yellow compound resulting from the decomposition under irradiation of the radical cation $MV^{\bullet+}$ by $O_2^{\bullet-}$ occurs (increase of the intensity at 535 nm) followed by the photodegradation of this emissive species (Scheme 1). The determination of the structure of the products resulting from the photodegradation of $V^{\bullet+}$ is outside the scope of this paper.[33,36a−d] The decomposition of the radical cation $MV^{\bullet+}$ is also evidenced by the decrease of its emission intensity at 325 nm (Figure 9, inset).

Consequently, the irradiation of dyad **1** in the presence of O_2 leads to the decomposition of the radical cation of the viologen units produced by intramolecular electron transfer from the excited ruthenium complex. This rules out the possibility

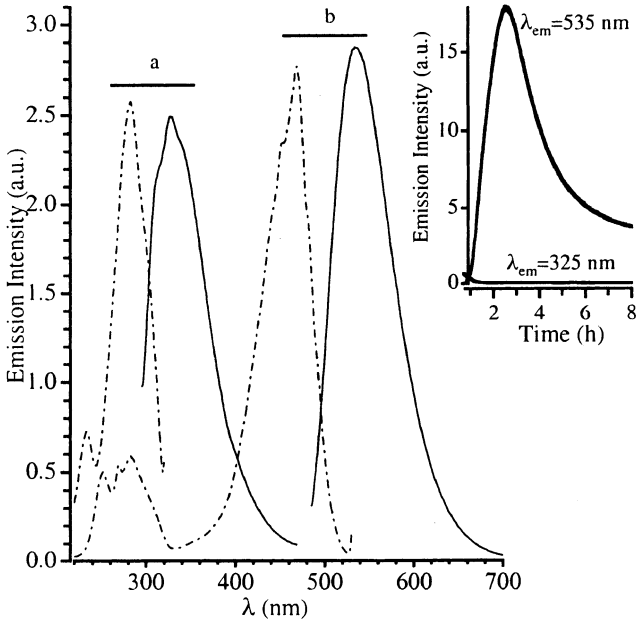

Figure 9. Emission (solid line) and excitation (dashed line) spectra of an acetonitrile solution of $MV^{\bullet+}$ (prepared in a glovebox under an argon atmosphere) recorded in the (a) absence or (b) presence of oxygen at room temperature. The excitation and emission wavelength are (a) λ_{em} = 325 nm and λ_{ex} = 284 nm and (b) λ_{em} = 535 nm and λ_{ex} = 470 nm. The inset shows the evolution of the emission intensity of $MV^{\bullet+}$ in acetonitrile solution containing air at 535 and 325 nm.

SCHEME 1: Schematic Mechanism of the Photodegradation of the Monoreduced Radical Cation of Viologen in the Presence of O_2

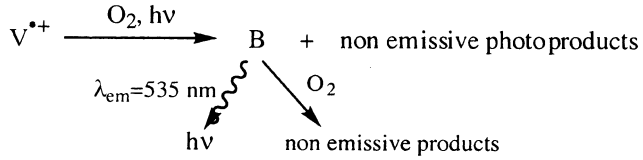

of a successful photopolymerization of dyad **1**. On the other hand, the decomposition process of the radical cation $V^{\bullet+}$ is slow. From Figure 9 (inset), the rate constant for this process has been estimated to be 1.4×10^{-3} s^{-1}·mol^{-1}·L. It can partly explain why this decomposition process is not observed in the case of dyad **2**. This evidences the deep importance of the separation distance between the excited ruthenium complex and the pyrrole groups for photopolymerization. Indeed, in the case of dyad **1**, the too long distance between the pyrrole groups and the Ru(III) species would prevent the first step of the photopolymerization, which is the electron transfer from pyrroles to Ru(III) according to Pyr−Ru(III)−$V^{\bullet+}$ → $Pyr^{\bullet+}$−Ru(II)−$V^{\bullet+}$ → polypyrrole−Ru(II)−$V^{\bullet+}$. This way of photopolymerization is restored in the case of dyad **2** due to the shorter pyrrole−Ru(III) distance.

C. Photopolymer Features. *C.1. Electrochemistry.* Redox properties of solutions of photopolymers (photopoly-**2**) were analyzed by cyclic voltammetry after addition of electrolyte (0.1 M TBAP). For the photopolymer prepared in the presence of diazonium salt, two successive reductive electrolyses are first needed to eliminate the slight excess of the diazonium salt and protons liberated by the polymerization of pyrrole groups. The first one is carried out at −0.60 V on a carbon felt working electrode, while the second one is carried out at −0.60 V on a platinum electrode. Figure 10 gives the cyclic voltammogram of both photopolymers. All the expected redox systems of the supramolecular complex are present, although those of the ligand

TABLE 3: MLCT Absorption Band Maxima (λ_{abs}^{max}), Luminescence Maxima (λ_{em}^{max}), and Luminescence Decay Times (τ) for Dyad 2 and the Model Compound 5 as Monomer and Photopolymer at 298 K in Deoxygenated Acetonitrile Solution[a]

		λ_{abs}^{max} (nm)	λ_{em}^{max} (nm)	$\phi_{photopolymer}/\phi_{monomer}$	τ (ns)	k_{CT} (s^{-1})
$[Ru(L_1)_2(L_5)]^{6+}$, dyad **2**	monomer	490	677	1	1.62	6.4×10^8
	photopolymer	491	685	0.96	<10	1.09×10^8
$[Ru(L_1)_2(L_6)]^{2+}$, **5**, model compound	monomer	478	668	1	1080	
	photopolymer	478	667	0.98	1070	

[a] The emission quantum yield of the photopolymer (photosynthesized in the presence of O_2) relative to that of the corresponding monomer ($\phi_{photopolymer}/\phi_{monomer}$) is indicated. The rate constants for the forward (k_{CT}) intramolecular electron-transfer process in dyad **2** (monomer) or in photopoly-**2** are presented.

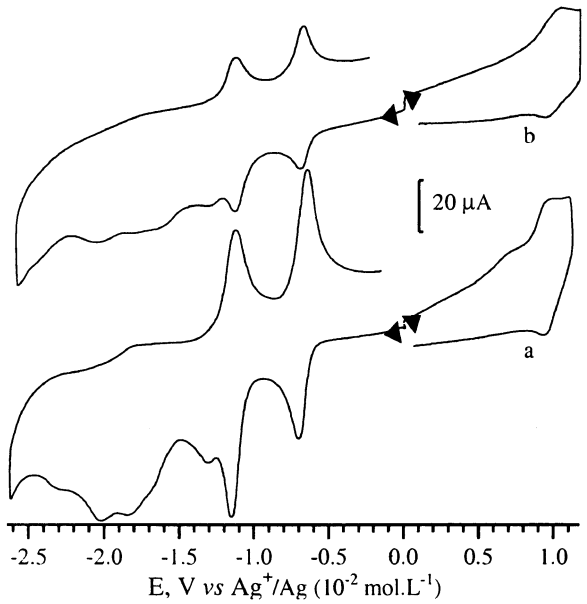

Figure 10. Cyclic voltammogram in CH_3CN/0.1 M TBAP at a C electrode, $\nu = 100$ mV s^{-1}, of photopoly-**2** (A) photosynthesized in the presence of diazonium salt as quencher and (B) photosynthesized in the presence of O_2 as quencher.

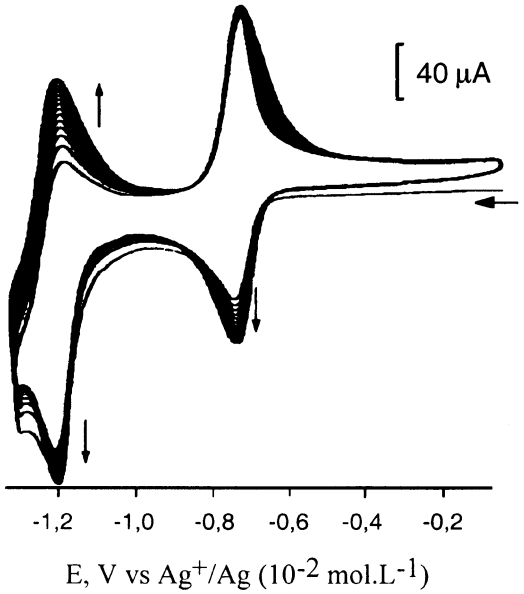

Figure 11. Electroreductive growth of a film from a solution of photopoly-**2** (prepared in the presence of O_2 as quencher) in CH_3CN/0.1 M TBAP by repeated scans at the reduction waves of the viologen moieties.

reductions appear broad due to some capacitive effect afforded by the polymeric matrix (see Table 1 for the potential data).

Repeated cycles in the negative region induce the continuous increase in size of the cyclic voltammetric peaks, indicating the accumulation of an electroactive film of photopoly-**2** on the electrode surface. Figure 11 shows the growth of a photopoly-**2** film by repeated scans over the two successive reduction waves of the viologen moieties. The poor solubility of the reduced forms of the polymerized complex is probably the main factor responsible for their adsorption at the electrode surface. Furthermore, in this potential range, the electrode is negatively charged and tetrabutylammonium countercations are concentrated in the double layer. Since these cations have a relatively hydrophobic nature, their interaction with the polymers might play an important role in the adsorption and the coverage of the electrode. A quite similar electroreductive precipitation phenomenon from soluble polypyrrole−ruthenium(II)−trisbipyridine complexes, not containing viologen groups, has been previously reported.[8,9] It is also important to emphasize that no similar coating was observed by continuous cycling of the potential in the same potential area of a solution of monomer **2**, showing that the deposition phenomenon is a consequence of the polymeric nature of photopoly-**2**. The resulting modified electrodes exhibit a stable electroactivity typical of the immobilized supramolecular complex after its transfer into CH_3CN + 0.1 M TBAP solution without initial complex (Figure 12; all the expected reversible peak systems of the viologens, bpy ligands, and metal reversible redox systems are observed). Their behavior is close to that of modified electrodes prepared by direct anodic electropolymerization of dyads **1** and **2** (Figure 2).

C.2. Photophysics. Despite the cross-linked character of the resulting polymer, the photopolymerization of dyad **2** does not lead to a significant change in its photophysical properties. Only a slight broadening of the absorption spectrum can be detected, as previously observed for Ru−polypyrrole systems not containing viologen units. The values of the quantum yield (Φ_L) exhibited by dyad **2** (monomer) and its corresponding photopolymer are similar (Table 3). The difference observed is rather marginal and close to the experimental error. Quite obviously, it appears that, in the polymer system, the individual Ru sites are largely isolated from an electronic point of view. Regarding the results previously obtained on $Ru(bpy)_3$–polypyrrole systems[10] and as the length of the alkyl chain between the Ru center and the pyrrole group is short, a significant change in Φ_L would be expected. This change is not observed, which suggests that the length of the polymer backbone is short. It would be perhaps more appropriate to consider the photopolymer of dyad **2** as a cross-linked oligomer rather than as a cross-linked polymer.

On the other hand, since the luminescence quantum yields and time decays are of the same order of magnitude for the photopoly-**2** and dyad **2** systems, the electron-transfer process from the excited Ru complex to the viologen units occurs in the polymer systems. This confirms that the photopolymerization of dyad **2** in the presence of O_2 does not induce a significant photodegradation of the viologen units.

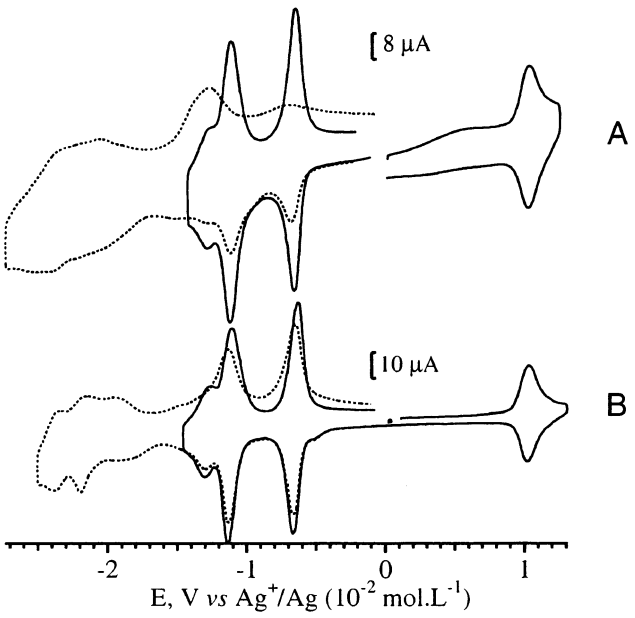

Figure 12. Cyclic voltammogram in CH_3CN/0.1 M TBAP, $\nu = 100$ mV s^{-1}, at a Pt/photopoly-**2**-modified electrode prepared by electroreductive coating, from a solution of photopoly-**2** prepared (A) by using a diazonium salt as quencher ($\Gamma = 1.1 \times 10^{-9}$ mol·cm^{-2}) and (B) by using O_2 as quencher ($\Gamma = 0.9 \times 10^{-9}$ mol·cm^{-1}).

Furthermore, the photochemical stability of the viologen units in the polymer systems has been checked by irradiation of an aerated solution of poly(dyad **2**) for more than 3 h. No significant change in the emission intensity at 666 nm has been detected.

Conclusion

In the present paper, we report the synthesis and the characterization of the first soluble polymer based on a polypyrrole−bisviologen-linked $[Ru(bpy)_3]^{2+}$ dyad. To achieve successful photopolymerization, the design of the dyad monomer appears to be crucial. An arrangement that consists of chemically separating the polymerizable pyrrole groups from the Ru center by the electron acceptor viologen units leads to the complete annihilation of the photopolymerization process.

On the other hand, from the photophysical measurements, the network appears to be not dense though the polymer is expected to be cross-linked and the distance between the Ru centers and the polymer backbone short. This suggests that the photopolymerization of the dyad investigated here leads mainly to cross-linked short oligomers.

Furthermore, the intramolecular electron transfer occurring from the photoexcited Ru complex to the viologen group is kept in the polymer system even when the photopolymerization is achieved in the presence of oxygen: the product of the photodegradation of the monoreduced viologen characterized by a short lifetime emission at 535 nm has not been detected. The photostability of the dyad network in the presence of oxygen opens the interesting possibility of the use of such a system for its application in photoinduced redox processes.

Supporting Information Available: Figure showing the proton NMR chemical shifts observed for dyads **1** and **2**. This material is available free of charge via the Internet at http://pubs.acs.org.

References and Notes

(1) Baxter, S. M.; Jones, W. E.; Danielson, E.; Worl, L.; Strouse, G. F.; Younathan, J.; Meyer, T. J. *Coord. Chem. Rev.* **1991**, *111*, 47−71.

(2) Balzani, V.; Scandola, F. In *Supramolecular Photochemistry*; Kemp, T. J., Ed.; Ellis Horwood: London, 1991; pp 89−150.

(3) Piotrowiak, P. *Chem. Soc. Rev.* **1999**, *28*, 143−150.

(4) Connolly, J. S.; Bolton, J. R. In *Photoinduced electron transfer*; Fox, M. A., Chanon, M., Eds.; Elsevier: New York, 1988; Part D, Chapter 6.2, pp 303−393.

(5) Matsuo, T.; Sakamoto, T.; Takuma, K.; Sakura, K.; Ohsako, T. *J. Phys. Chem. A* **1981**, *85*, 1277−1279.

(6) Younathan, J. N.; Jones, W. E.; Meyer, T. J. *J. Phys. Chem. A* **1991**, *95*, 488−492.

(7) Suzuki, M.; Kimura, M.; Hanabusa, K.; Shirai, H. *Polymer* **1999**, *40*, 3971−3978.

(8) Deronzier, A.; Jardon, P.; Martre, A.; Moutet, J.-C.; Santato, C.; Balzani, V.; Credi, A.; Paolucci, F.; Roffia, S. *New J. Chem.* **1998**, 33−37.

(9) Deronzier, A.; Eloy, D.; Jardon, P.; Martre, A.; Moutet, J.-C. *J. Electroanal. Chem.* **1998**, *453*, 179−185.

(10) Laguitton-Pasquier, H.; Martre, A.; Deronzier, A. *J. Phys. Chem. B* **2001**, *105*, 4801−4809.

(11) Deronzier, A.; Essakali El-Hocini, M. *J. Chem. Soc., Chem. Commun.* **1990**, 242−244.

(12) Cosnier, S.; Deronzier, A.; Moutet, J.-C. *J. Electroanal. Chem.* **1985**, *193*, 193−204.

(13) Sprintschnick, G. H. W.; Kirsch, P. P.; Whitten, D. G. *J. Am. Chem. Soc.* **1977**, *99*, 4947−4954.

(14) Collomb, M.-N.; Deronzier, A.; Ziessel, R. *J. Phys. Chem.* **1993**, *97*, 5973−5979.

(15) Sullivan, B. P.; Salmon, D. J.; Meyer, T. J. *Inorg. Chem.* **1978**, *17*, 3334−3341.

(16) De Giovani, W. F.; Deronzier, A. *J. Chem. Soc., Chem. Commun.* **1992**, 1461−1463.

(17) Christensen, P. A.; Hamnett, E. A. *Electrochim. Acta* **1991**, *36*, 1263−1286.

(18) Douglas, R. J.; Siemiarczuk, A.; Ware, W. R. *Rev. Sci. Instrum.* **1992**, *63*, 1710−1716.

(19) Marquardt, D. W. *J. Soc. Ind. Appl. Math.* **1963**, *11*, 431−441.

(20) El-ghayoury, A.; Harriman, A.; Ziessel, R. *J. Phys. Chem. A* **2000**, *104*, 7906−7915.

(21) Rutherford, T. J.; Reistma, D. A.; Keene, F. R. *J. Chem. Soc., Dalton Trans.* **1994**, 3659−3666.

(22) Cosnier, S.; Deronzier, A.; Rolland, J.-F. *J. Electroanal. Chem.* **1990**, *285*, 133−147.

(23) Roundhill, D. M. *Photochemistry and Photophysics of Metal Complexes*; Plenum Press: New York, 1994; pp 165−215.

(24) Kalyanasundaram, K. *Coord. Chem. Rev.* **1982**, *46*, 159−244.

(25) Elliott, C. M.; Freitag, R. A.; Blaney, D. D. *J. Am. Chem. Soc.* **1985**, *107*, 4647−4655.

(26) Watanabe. T.; Honda, K. *J. Phys. Chem.* **1982**, *86*, 2617−2619.

(27) Morris, D. E.; Hanck, K. W.; Keith de Armond, M. *J. Am. Chem. Soc.* **1983**, *105*, 3032−3038.

(28) Keith De Armond, M.; Myrrick, M. L. *Acc. Chem. Res.* **1989**, *22*, 364−370.

(29) Kelly, L. A.; Rodgers, M. A. *J. Phys. Chem.* **1995**, *99*, 13132−13140.

(30) In agreement with our experimental results (both dyads exhibit the same lifetime, k_{CT} and k_b, values), no supplementary quenching processes are expected in the case of dyad **2**. Indeed, as previously shown,[10] the alkylpyrrole chain does not induce a significant quenching of the ^{3}MLCT-Ru^{2+}* excited state. Furthermore, a quenching by the pyrrole group of the Ru(III)−$V^{\bullet+}$ charge-transfer state would lead to photopolymerization not observed without the addition of an irreversible oxidative quencher.

(31) Hiraishi, T.; Kamachi, T.; Okura, I. *J. Photochem. Photobiol., A* **1998**, *116*, 119−125.

(32) Yonemoto, E. H.; Rilley, R. L.; Il Kim, Y.; Atherton, S. J.; Schmehl, R. H.; Mallouk, T. E. *J. Am. Chem. Soc.* **1992**, *114*, 8081−8087.

(33) Clark, C. D.; Debad, J. D.; Yonemoto, E. H.; Mallouk, T. E.; Bard, A. J. *J. Am. Chem. Soc.* **1997**, *119*, 10525−10531.

(34) Chen, Z.-K.; Meng, H.; Lai, Y.-H.; Huang, W. *Macromolecules* **1999**, *32*, 4351−4358.

(35) The lifetimes of the species emitting at 546 and 535 nm estimated from the decay curves are similar and amount to less than 10 ns.

(36) See the following references for further information concerning the toxicity of the monoreduced radical cation of viologen in the presence of air: (a) Calderbank, A.; Charlton, D. F.; Farrington, J. A.; James, R. *J. Chem. Soc., Perkin Trans. 1* **1972**, *1*, 138−142. (b) Nanni, E. J.; Angelis, C. T.; Dickson, J.; Sawyer, D. T. *J. Am. Chem. Soc.* **1981**, *103*, 4268−4270. (c) Forster, M.; Hester, R. E. *J. Chem. Soc., Faraday Trans. 1* **1982**, *78*, 1847−1866. (d) Shelepin, I. V.; Barachevskii, V. A.; Kunavin, N. I. *Russ. J. Phys. Chem.* **1975**, *49*, 1019−1021.